Materials and Structures (2021)54:225
https://doi.org/10.1617/s11527-021-01812-9

ORIGINAL ARTICLE

Experimental assessment and modeling of fracture and fatigue resistance of aged stone matrix asphalt (SMA) mixtures containing RAP materials and warm-mix additive using ANFIS method

Seyed Ataollah Saed · Neda Kamboozia · Hassan Ziari · Bernhard Hofko

Received: 2 June 2021 / Accepted: 26 October 2021

Abstract In this research, the fracture and fatigue resistance of short and long-term aged hot and warm mix (HMA and WMA) stone matrix asphalt (SMA) mixtures containing 0%, 30%, 40%, and 50% RAP materials were investigated using semi-circular bending (SCB) and four-point beam fatigue (4 PB) test methods. It is further noted that three temperatures (− 20 °C, 0 °C, and 20 °C) were considered for the SCB test to take the viscoelastic behavior of asphalt mixtures into account. The adaptive neuro-fuzzy interface system (ANFIS) method was utilized to model the fracture and fatigue parameters obtained from each test so as to cut back on the time and cost for conducting the tests. The results indicated that the incorporation of RAP materials into HMA mixtures decreased the fatigue life and fracture resistance as compared to the control mixture at lower temperatures, even though an increase in the fracture resistance was observed at the intermediate temperature. It is further noted that the addition of WMA additive into SMA mixtures containing 50% RAP materials resulted in a better fracture resistance as compared to the control mixture. However, the WMA additive incorporation led to shorter fatigue lives as compared to the corresponding HMA mixtures. Moreover, although long-term aging reduced the fracture resistance of HMA mixtures, its application resulted in a better fracture resistance in WMA mixtures. Also, long-term aging had a less adverse effect on the fatigue life of WMA mixtures as compared to HMA mixtures. It was also observed that the ANFIS model could estimate the fracture and fatigue parameters with great precision.

Keywords Reclaimed asphalt pavement (RAP) · Stone matrix asphalt (SMA) · Warm-mix asphalt (WMA) · Long-term aging · Short-term aging · Adaptive neuro-fuzzy interface system (ANFIS)

1 Introduction

The construction or rehabilitation of asphalt pavements requires plenty of aggregates and asphalt binders. The recycling of reclaimed asphalt pavement (RAP) has contributed to lessening the environmental and economic problems associated with the construction or rehabilitation of asphalt pavements with solely virgin materials [1, 2]. It was found by researchers that due to the fact that the addition of RAP materials into asphalt mixtures increases the stiffness, the rutting resistance of mixtures with RAP materials is higher

S. A. Saed · N. Kamboozia (✉) · H. Ziari
School of Civil Engineering, Iran University of Science and Technology (IUST), Tehran 16846-13114, Iran
e-mail: nkamboozia@iust.ac.ir

B. Hofko
Institute of Transportation, Vienna University of Technology, Vienna, Austria

Published online: 20 November 2021

than the reference mixture [3]. In addition, due to the strong bonding between aggregates and asphalt binder in highly aged RAP materials, asphalt mixtures with RAP materials have better resistance against moisture damages [4].

It is axiomatic that the addition of RAP materials into asphalt mixtures has a significant effect on the fatigue and fracture resistance of mixtures. It was reported by researchers that the fatigue resistance of asphalt mixtures containing RAP materials is lower than the reference mixture [5]. Besides, although Ziari et al. [6] reported that the fracture resistance of asphalt mixtures was decreased by incorporating RAP materials at intermediate temperature, Yousefi et al. [7] and Saed et al. [8] reported a higher fracture resistance of asphalt mixtures containing RAP materials at intermediate temperature.

The advent of warm mix asphalt (WMA) additives has significantly reduced energy consumption and greenhouse gas emissions. Apart from environmental benefits, asphalt mixtures produced by WMA additives have several technical advantages and disadvantages. Different studies showed that the rutting, fracture, and fatigue resistance of asphalt mixtures could be improved by the addition of Sasobit® WMA additive to asphalt mixtures [7, 9, 10]. As for fatty acid amides, Rodríguez-Alloza and Gallego [11] reported that the addition of Licomont BS100® WMA additive to asphalt mixtures increased the rutting resistance. Yousefi et al. [7] observed that the WMA mixtures produced by Kaowax® and Pawma® WMA additives have better rutting and fracture resistance while the addition of Zeolite® WMA additive deteriorated the rutting resistance. Lu and Saleh [12] reported that the rutting and fatigue resistance of WMA mixtures fabricated by Evotherm® WMA additive are lower than HMA mixtures. In addition, due to the lower mixing and compaction temperatures in WMA mixtures, the adhesion between aggregates and asphalt binder might not be as strong as HMA mixtures; so, their moisture susceptibility might increase [13].

With the development of different prediction models, such as artificial neural network (ANN), group method of data handling (GMDH), and adaptive network-based fuzzy interface system (ANFIS), the high cost and time associated with conducting experimental tests have been reduced significantly [14]. Ziari et al. [14] observed that the precision of the ANFIS method in predicting the fracture resistance of fiber-modified asphalt mixtures with RAP materials was superior to the GMDH method. Alas et al. [15] concluded that the ANFIS method was incredibly reliable in predicting the G^* values of polymer-modified asphalt binders.

As can be seen in the literature, only a limited number of studies have been conducted to investigate the fracture resistance of WMA mixtures at relatively broad temperature ranges to take the viscoelastic behavior of asphalt mixtures into account. In addition, the effectiveness of additives might undergo a significant change during the service time of pavements. This requires researchers to take the long-term performance of asphalt mixtures into consideration. To the best of the authors' knowledge, far too limited studies have been performed to characterize the short and long-term fracture and fatigue properties of HMA and WMA mixtures containing RAP materials. To fulfill this gap in this research, the fatigue and fracture properties of short and long-term aged HMA/WMA mixtures containing RAP materials were investigated. Also, in order to take the visco-elastic behavior of asphalt mixtures into account, three temperatures (− 20 °C, 0 °C, and 20 °C) were chosen to investigate the fracture properties. Since the preparation and testing procedures are costly and time-consuming, the ANFIS prediction model was developed to estimate the fracture and fatigue properties of the aforementioned asphalt mixtures in order to the ease of asphalt mix designers.

2 Materials

2.1 Base binder

The asphalt binder used in this study was PG 64-22 obtained from a qualified oil company, and its properties are presented in Table 1. The reason for selecting this binder was that its performance grade corresponds to the temperature variations that are dominant in many regions.

2.2 Aggregate

In this research, the limestone aggregates were used, and their properties were checked to be placed within the acceptable criteria as per the recommendations of

Table 1 Physical properties of the base binder, RAB, and aggregates

Features	Unit	Standard	Criteria	Results
Base binder				
Rotational viscosity at 135 °C	Pa.s	ASTM D4402	≤ 3	0.35
Penetration	0.1 mm	ASTM D5	60–70	64
Ductility	cm	ASTM D113	≥ 100	104
Softening point	°C	ASTM D36	≥ 46	49
Specific gravity	g/cm^3	ASTM D70		1.016
Flash point	°C	ASTM D92	≥ 235	304
Solubility in trichloroethylene	%	ASTM D2042	> 99	99.7
Mass loss	%	ASTM D1754	< 1	0.11
$G^*/\sin\delta$ @ 64 °C (Original)	KPa	ASTM T315	≥ 1	1.408
$G^*/\sin\delta$ @ 64 °C (RTFO-aged)	KPa	ASTM T315	≥ 2.2	2.561
RAB				
Rotational viscosity at 135 °C	Pa.s	ASTM D4402	–	2.76
Penetration	0.1 mm	ASTM D5	–	31
Ductility	cm	ASTM D113	–	7.2
Softening point	°C	ASTM D36	–	59
$G^*/\sin\delta$ @ 64 °C (original)	KPa	ASTM T315	–	6.014
$G^*/\sin\delta$ @ 64 °C (RTFO-aged)	KPa	ASTM T315	–	12.791
Coarse aggregates (> 4.75 mm)				
Los angeles abrasion	%	AASHTO T96	≤ 30	23
Flat and elongated (3 to 1)	%	ASTM D4791	≤ 20	8
Flat and elongated (5 to 1)	%	ASTM D4791	≤ 5	0.8
Absorption	%	AASHTO T85	≤ 2	1.2
Soundness(5 cycles), Sodium sulfate	%	AASHTO T104	≤ 15	0.2
Crushed content, one face	%	ASTM D5821	100	100
Crushed content, two face	%	ASTM D5821	≥ 90	100
Fine aggregates (< 4.75 mm)				
Soundness(5 cycles), Sodium sulfate	%	AASHTO T104	≤ 15	1.0
Liquid limit	%	AASHTO T89	≤ 25	18
Plasticity index	%	AASHTO T90	Non-plastic	Non-plastic
Sand equivalent	%	AASHTO T176	–	84

AASHTO M325-08 [16]. The aggregates' properties are presented in Table 1.

2.3 RAP material

In this study, RAP materials were obtained from the milling and crushing process on a highway, which had been under service without being rehabilitated for 8 years. The RAP binder was extracted and recovered as per the procedures prepared by ASTM D2172M-17 [17] and ASTM D5404M-12 [18]. The gradation of the RAP materials' aggregate and the properties of the RAP binder were ascertained and presented in Fig. 1 and Table 1, respectively.

2.4 Cellulose fiber

In this study, a cellulose fiber at the content of 0.3% by the weight of the total mixture mass was utilized to prevent draindown, according to AASHTO M325-08 [16]. Cellulose fiber was directly incorporated into asphalt mixtures [19].

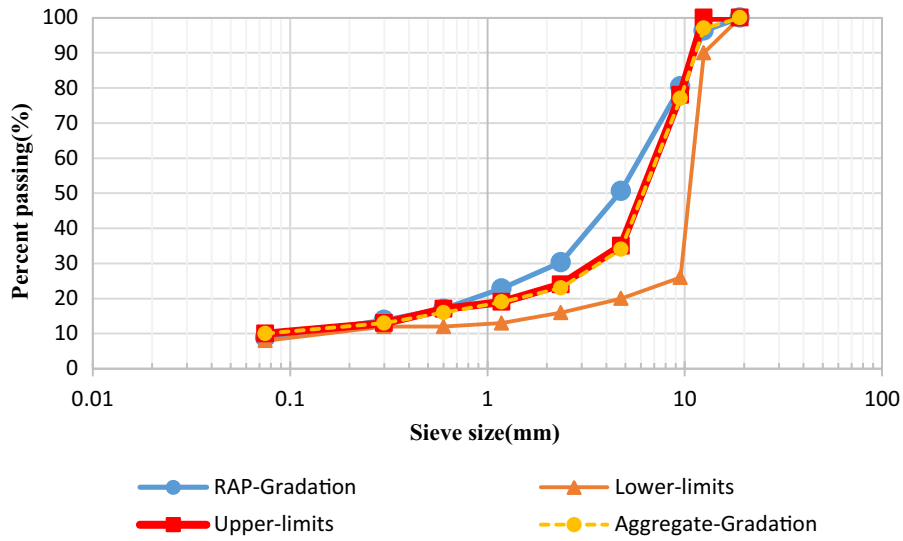

Fig. 1 The gradation of the RAP materials and aggregates

2.5 WMA additive

WMA additive used in this study was an organic wax named Sasobit®. It is categorized as one of the commonly adopted WMA additives that have an average melting temperature of 100 °C [10]. It was added to the base binder at the content of 3% by the weight of the total binder mass, which was also used at this content by previous studies [20, 21].

3 Methodology

3.1 Mixing and compaction temperatures

In this study, unique codes were assigned to the corresponding mixtures so as to make the report and discussion more accessible. In this vein, short-term aged control HMA and WMA mixtures were shown by abbreviations of "C" and "WC," respectively. Long-term aged control HMA and WMA mixtures were abbreviated by "LC" and "LWC," respectively. The content of RAP materials in each mixture was shown by a percentage at the end of acronyms. For example, LWC30 indicates a long-term aged WMA mixture containing 30% RAP materials.

The mixing and compaction temperatures correspond to rotational viscosities of 0.17 Pa ± 0.02.s and 0.28 Pa ± 0.03.s, respectively [22]. The base binder, WMA binder, and RAP binder were intermixed at ratios corresponding to those of asphalt mixtures. Afterward, the rotational viscosity test was performed on each binder compound at temperatures of 110 °C, 135 °C, 150 °C, and 165 °C, according to AASHTO T316-19 [23]. Then, the mixing and compaction temperatures were determined and presented in Table 2.

3.2 Mixing WMA additive into the base binder

Previous studies demonstrated that the Sasobit® is mixed into the binder at temperature ranges between 135 and 150 °C using a low-shear mixer with the rotation speed of 300 to 500 rpm, continuing for 10–15 min [24, 25]. Therefore, in this study, the base binder was heated to the temperature of 140 °C Then, 3% Sasobit® by the weight of the total binder was added to the base binder and mixed at the rotation speed of 400 rpm, continuing for 15 min using a low-shear mixer.

3.3 Mix design of SMA mixtures

The gradation of SMA mixtures adopted in this study had the nominal maximum aggregate size of 12.5 mm, which was selected as per the recommendations of AASHTO M325-08 [16] (see Fig. 1).

Virgin aggregates and RAP materials were kept at mixing temperatures for 16 and 2 h, respectively. Afterward, virgin aggregates, RAP materials, and cellulose fiber were mixed together, followed by adding the varying contents of the virgin base binder

Table 2 Mixing and compaction temperatures of asphalt mixtures

Asphalt mixture code*	Mixing temperature (°C)	Compaction temperature (°C)
C	150	140
C30	161	145
C40	163	150
C50	165	152
WC	132	125
WC30	149	134
WC40	153	140
WC50	156	145

*No aging was implemented on asphalt binders, which rotational viscosity test was performed on

so as to determine the optimum binder content of SMA mixtures containing 0%, 30%, 40%, and 50% RAP materials. Then, uncompacted mixtures were compacted using the Marshall method [26]. Finally, the optimum virgin base binder contents of SMA mixtures containing 0%, 30%, 40%, and 50% RAP materials were ascertained as 6.1%, 4.2%, 3.7%, and 3.4%, respectively, according to AASHTO T245-15 [26] and additional requirements mentioned for SMA mixtures in AASHTO R46-08 [27].

As mentioned previously, short and long-term properties of asphalt mixtures were assessed by the laboratory aging mechanism. All uncompacted mixtures considered for the SCB and 4 PB tests were placed at the temperature of 135 °C for 4 h in order to simulate the short-term aging as per the recommendations of AASHTO R30-02 [28]. With regard to simulating the long-term aging, compacted mixtures were placed at the temperature of 85 °C for 120 h, according to AASHTO R30-02 [28].

4 Test methods

4.1 Semi-circular bending (SCB) test

For fabricating SCB specimens, asphalt mixtures were compacted to the target air void with three replicates under the same condition using a gyratory compactor, according to ASTM D8044-16 [29]. Then, the fabricated cylindrical specimens were cut and halved into SCB specimens having notch depths of 25, 32, and 38 mm as per the guidelines prepared by ASTM D8044-16 [29]. Afterward, all specimens were held at the testing temperatures, including − 20 °C, 0 °C, and 20 °C, for 4 h before the initiation of the test. The reason for selecting these temperatures is to take the viscoelastic behavior of asphalt mixtures into account. Then, the test was initiated by applying a constant loading rate of 0.5 mm/min using a universal testing machine (UTM). The specimens and test setup are shown in Fig. 2.

The fracture properties of asphalt mixtures were investigated using fracture energy (Eq. (1)) and critical J-integral (Eq. (2)) parameters in accordance with ASTM D8044-16 [29].

$$G_f = \frac{U}{L} = \int (P) du / dL \tag{1}$$

where G_f = Fracture energy until failure point (J/m^2); L = Unit area of the ligament (m^2); and U = Strain energy (J).

$$J_C = -\left(\frac{1}{b}\right)\left(\frac{dU}{da}\right) \tag{2}$$

where J_C = Critical J-integral (J/m^2); a = Notch depth (mm); b = Specimen thickness (mm); and U = Strain energy (J).

4.2 Four-point beam fatigue (4 PB) test

The flexural beams were fabricated to the target air void with three replicates under the same condition using a Roller Wheel compactor as per the stages mentioned in AASHTO T321 [30]. This test was conducted at a loading frequency of 10 Hz at the strain levels of 500, 600, 700, and 800 με at the temperature of 20 °C as per the guidelines prepared by AASHTO T321 [30]. Consequently, the fatigue life of mixtures was determined according to the mentioned specification. The specimens and test setup are shown in Fig. 2.

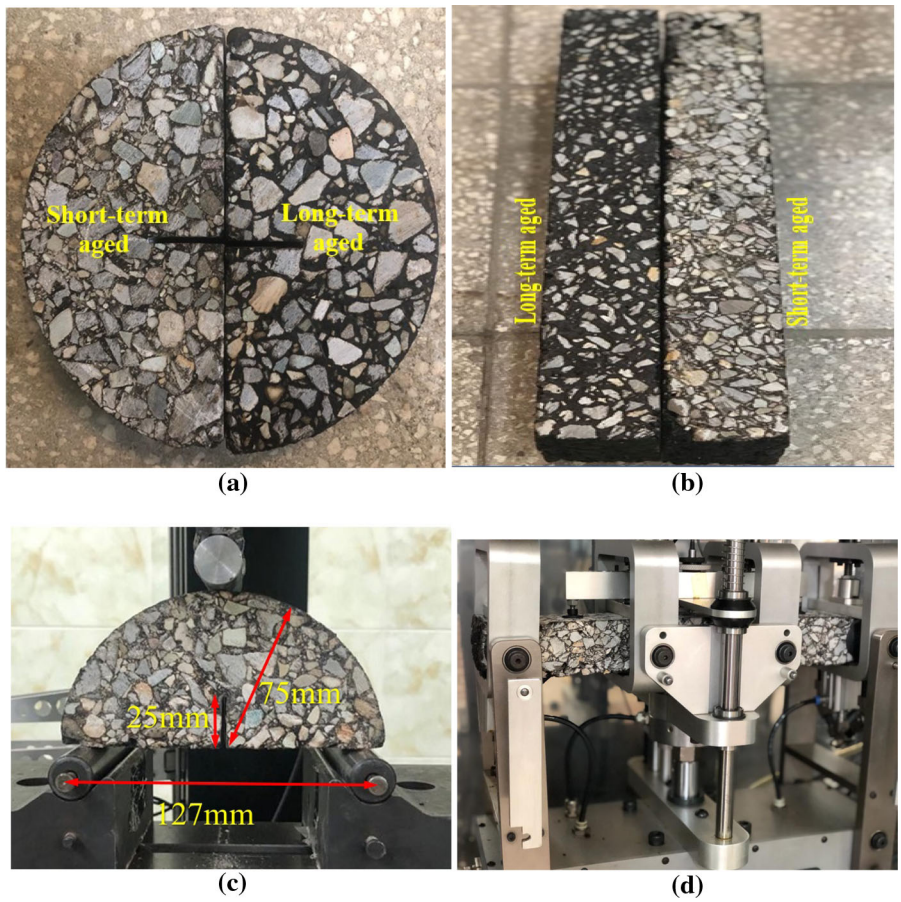

Fig. 2 Specimens and test setups: **a** SCB specimens; **b** 4 PB specimens; **c** SCB test setup; and **d** 4 PB test setup

4.3 The ANFIS prediction model

This method comprises several nodes and links. The functions are assigned in nodes, and links connect the nodes together [15]. This method consists of five layers. In layer 1, the function of nodes is determined using Eqs. (3) and (4). In layer 2, the firing strength of a rule is represented by multiplying the input signals by node function so as to act as the output signals (Eq. (5)) [14]. In layer 3, the output of i is divided by the sum of all outputs so that the node output be normalized (Eq. (6)). In layer 4, the fuzzy if–then rules are multiplied by the normalized output (Eq. (7)). Finally, In layer 5, the overall output can be derived by utilizing the Eq. (8).

$$O_{1.i} = \mu A_i(x) \text{ for i} = 1, 2 \tag{3}$$

$$O_{1.i} = \mu B_i(y) \text{ for i} = 3, 4 \tag{4}$$

$$O_{2.i} = \mu A_i(x) \times \mu B_i(y) = W_i \text{ for i} = 1, 2 \tag{5}$$

$$O_{3.i} = \frac{W_i}{\sum W_i} \text{ for i} = 1, 2 \tag{6}$$

$$O_{4.i} = \overline{W_i} \times f_i \quad for\, i = 1, 2 \tag{7}$$

$$O_{5.i} = \sum_i \overline{W_i} \times f_i = \frac{\sum_i W_i f}{\sum_i W_i} \tag{8}$$

For training, validating, and testing the data, the fuzzy interface system was developed using the fuzzy logic tool in MATLAB software. In this research, the grid partitioning method using the gaussmf membership function type was used to generate the fuzzy interface system. It should be noted that the ANFIS method does not assign the number of membership functions automatically; so, several numbers of

membership functions were tested for every input in order to boost the model precision.

5 Results and discussion

5.1 SCB test results

Effect of RAP addition Fracture energy indicates the external energy required for reaching the failure point, and crack propagation resistance of asphalt mixtures is characterized by J-integral values. Fracture energy and J-integral values of different compounds of mixtures are depicted in Figs. 3 and 4, respectively. As can be seen in Figs. 3a, b, and 4, HMA mixtures containing 40% and 50% RAP materials (C40 & C50) have lower fracture energy and J-integral values as compared to the control mixture (C) at temperatures of 0 °C and − 20 °C. This trend was also observed in a study conducted by Behnia et al. [31]. However, contradicting results were also reported [14]. However, HMA mixtures containing 30% RAP materials (C30) have higher fracture energy and J-integral values at the temperature of − 20 °C as compared to the control mixture (C). It is further noted that the fracture energy and J-integral values of HMA mixtures with RAP materials (C30-C50) are higher than the control mixture (C) at 20 °C. This trend was also reported by previous studies [7, 32]. Ziari et al. [14], however, reported contradicting results.

It can be deduced that the crack propagation resistance and the need for additional external energies are decreased by the addition of RAP materials at lower temperatures (i.e., 0 °C and − 20 °C). Conversely, the crack propagation resistance of HMA mixtures is increased by adding RAP materials at intermediate temperature (i.e., 20 °C).

The changes in fracture energy values of mixtures with 40% and 50% RAP materials at 0 °C and − 20 °C can be explained by the fact that at these temperatures, the level of displacements in asphalt mixtures is extremely low, which is intensified after the addition of RAP materials. This implies that at low temperatures, the fracture energy values are mostly dependent upon displacements rather than maximum loads. Hence, a substantial decrease in the displacements after the addition of RAP materials results in lower fracture energy values as compared to the control mixture. On the other hand, at the intermediate temperature, the fracture energy values of asphalt mixtures are highly dependent upon the maximum load values rather than displacements. As the addition of RAP materials increases the load-bearing capacity of mixtures, the fracture energy values increase after the addition of RAP materials at intermediate temperature.

The better crack resistance of mixtures with RAP materials at 20 °C can be attributed to the formation of coated layered particles after the addition of RAP materials [33]. It is axiomatic that the aged asphalt binder in RAP materials is well-dispersed within the aggregate particles rather than being just adsorbed by the aggregates' surface. This shows that the adhesion between the asphalt binder and aggregates in RAP materials is strong enough that the external energy required for debonding is high. Therefore, the crack resistance of mixtures with RAP materials increases at intermediate temperatures due to the delay in the microcrack formations before reaching the failure point.

Effect of WMA addition As shown in Figs. 3 and 4, WMA mixtures have lower fracture energy and J-integral values as compared to the corresponding HMA mixtures at any given temperature, with the only exception that the WMA mixture with 50% RAP materials (WC50) has higher J-integral values as compared to its HMA counterpart (C50) at − 20 °C. This finding was also reported by a study conducted by Singh et al. [32]. Yousefi et al. [7], on the other hand, reported contradicting results.

The changes in the fracture energy and J-integral values of mixtures after the addition of the WMA additive indicate that the addition of the WMA additive decreases the need for additional external energies to reach the failure point and also decreases the crack propagation resistance of asphalt mixtures. It is further noted that since the asphalt mixture is categorized as a heterogeneous multi-phase material, its fracture performance relies upon the constituents, such as the adhesion between the asphalt binder and aggregates and the cohesive force of asphalt binder [34]. It can be deduced that since the fracture performance of asphalt mixtures is affected by the addition of WMA additive, the addition of Sasobit® has a significant effect on the adhesion between the asphalt binder and aggregates and the cohesion force of the asphalt binder.

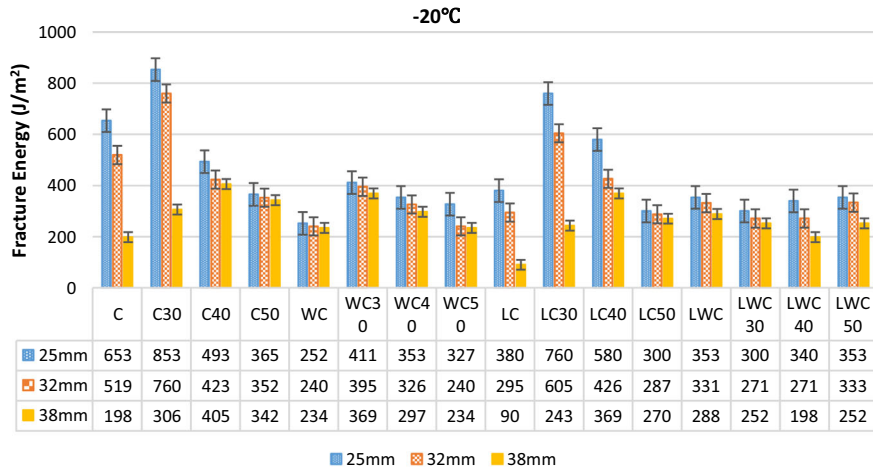

(a)

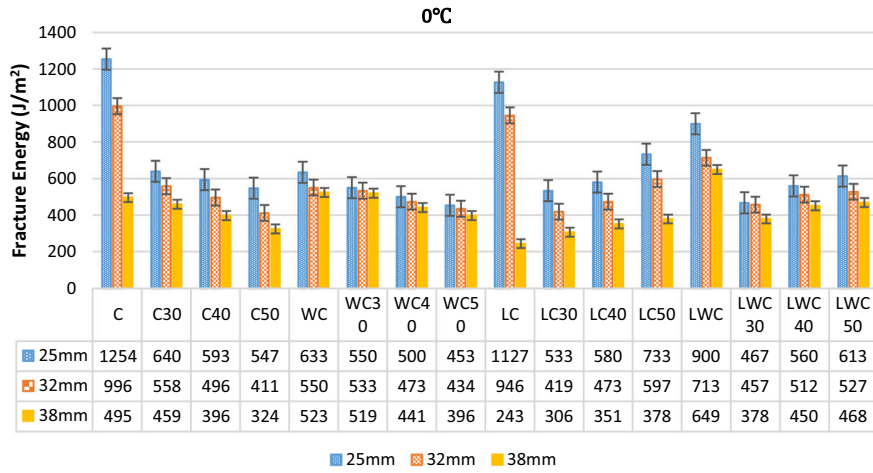

(b)

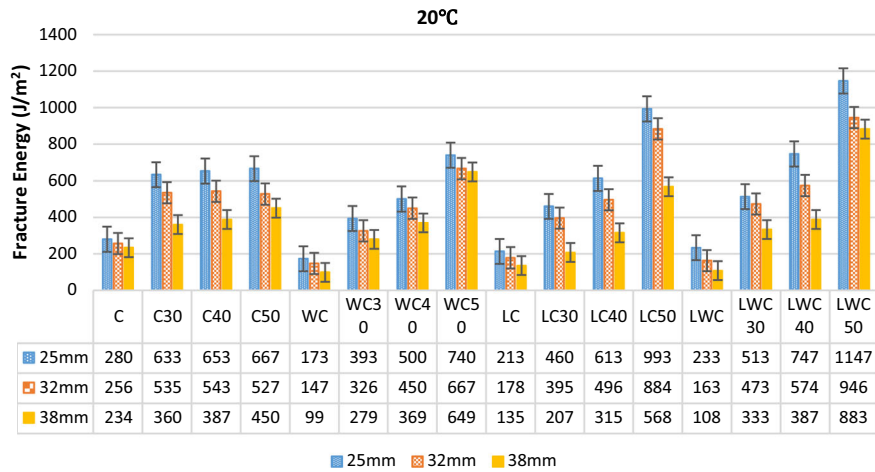

(c)

Fig. 3 Fracture energy values of different compounds of SMA mixtures: **a** − 20 °C; **b** 0 °C; and **c** 20 °C

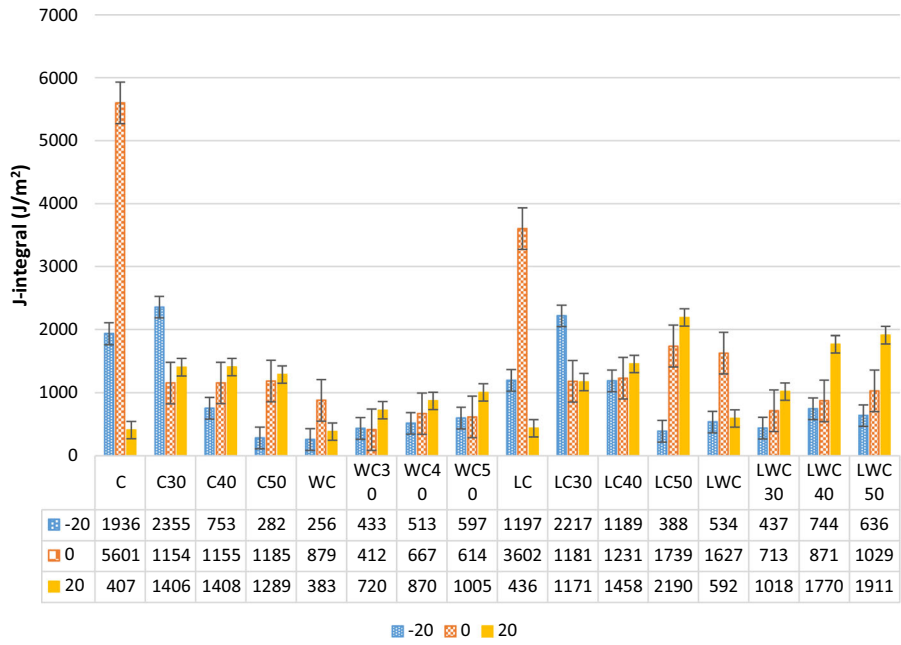

	C	C30	C40	C50	WC	WC30	WC40	WC50	LC	LC30	LC40	LC50	LWC	LWC30	LWC40	LWC50
-20	1936	2355	753	282	256	433	513	597	1197	2217	1189	388	534	437	744	636
0	5601	1154	1155	1185	879	412	667	614	3602	1181	1231	1739	1627	713	871	1029
20	407	1406	1408	1289	383	720	870	1005	436	1171	1458	2190	592	1018	1770	1911

Fig. 4 J-integral values of different compounds of mixtures

Wasiuddin et al. [35] reported that, in general, the addition of Sasobit® decreases the adhesion between asphalt binder and aggregates [35]. This can be attributed to a reduction in the viscosity of the asphalt binder after the addition of the WMA additive [36]. According to a study conducted by Guo et al. [37], lower viscosity values of asphalt binder result in a decrease in the bonding between the aggregates and the asphalt binder. Hence, the poorer adhesion between the aggregates and the WMA binder leads to less need for additional external energies to reach the failure point as compared to HMA mixtures. In addition, Li et al. [38] reported that since the Sasobit® is a long-chain aliphatic polymethylene hydrocarbon produced by the Fischer–Tropsch procedure using the natural gas, its addition to the asphalt binder decreases the cohesion force. As a result, the coupled detrimental effects of Sasobit® addition on the adhesion and cohesion strength lead to the poorer fracture resistance of mixtures.

As mentioned in the above paragraphs, WMA mixture containing 50% RAP materials (WC50) has a higher J-integral value as compared to its corresponding HMA mixture (C50) at − 20 °C. This shows that the use of WMA additive in combination with high contents of RAP materials (i.e., 50% RAP) is advantageous to the cracking resistance of mixtures at cold regions. This can be explained by the fact that the sensitivity of asphalt mixtures with 50% RAP materials to the strain energy is increased by the addition of WMA additive at lower temperatures, which accordingly results in an increase in the critical J-integral value.

Effect of aging As shown in Figs. 3 and 4, long-term aged HMA mixtures containing 0%, 30%, and 40% RAP contents (LC-LC40) have lower fracture energy and J-integral values as compared to the corresponding short-term aged mixtures (C-C40) at any given temperature, even though HMA mixture containing 50% RAP materials (C50) is an exception to this behavior at 0 °C and 20 °C. This shows that the aging mechanism decreases the crack propagation resistance of HMA mixtures. This can be due to the fact that aging increases the interconnected voids throughout asphalt mixtures [39], which in turn leads to a decrease in the durability of asphalt mixtures regarding fracture resistance. This is because when the pores are connected together, they extend within the structure of samples. As a result, the overall imperfection of mixtures regarding the fracture resistance is increased after being subjected to long-term aging.

With regard to the fracture resistance of long-term aged HMA mixture with 50% RAP materials (LC50),

it is observed that its fracture resistance goes higher after long-term aging. This can be explained by the fact that the aging increases the slope of the strain energy versus notch depths' linear regression. This, in turn, results in increasing the susceptibility of this mixture against the changes in the notch depths and strain energies. So, the J-integral value for this mixture is increased by the application of aging. It can be concluded that the adoption of RAP materials in high contents is favorable in terms of aging resistance.

As shown in Fig. 4, long-term aging had a less adverse effect on the fracture resistance of HMA mixtures with RAP materials as compared to the control mixture. This shows that the aging resistance of HMA mixtures with RAP materials is better than the control mixture in terms of fracture resistance. This is because the aging mechanism has been adequately applied to RAP materials during their service time, and further aging has an insignificant effect on the functional groups of the RAP binder.

As shown in Fig. 4, in general, long-term aging does not have an adverse effect on the fracture resistance of WMA mixtures. This can be explained by the fact that the resistance of the WMA binder along with the RAP binder against cohesion fracture is enhanced by aging [40]. Moreover, this finding is hypothesized by that the aged RAP binder and WMA binder interact more easily in WMA mixtures than HMA mixtures during long-term aging, which can be due to the lower viscosity of the WMA binder. As a result, asphalt binder film thickness is increased by getting plenty of asphalt binder peeled off the RAP materials after the addition of WMA additive [37]. Consequently, the adoption of WMA additive in combination with RAP materials is advantageous to the long-term fracture resistance of asphalt mixtures.

5.2 Four-point beam fatigue test results

Effect of RAP addition Fatigue life values of different compounds of mixtures are illustrated in Fig. 5. As can be seen in the corresponding figure, the fatigue life of mixtures with RAP materials is highly dependent upon the strain level. This means that HMA mixtures with RAP materials (C30-C50) have lower fatigue lives at the strain levels below 800 $\mu\varepsilon$ as compared to the control mixture (C), whereas the fatigue lives of these mixtures are higher than the control mixture at the strain level of 800 $\mu\varepsilon$. Zhang et al. [3] also reported the lower fatigue life of mixtures with RAP materials at the strain level of 100 $\mu\varepsilon$. In another study conducted by Bharath et al. [41], it was reported that the addition of RAP materials leads to a decrease in the fatigue life of asphalt mixtures, according to the results of indirect tensile fatigue test in the stress-controlled mode.

The above-mentioned trend in the fatigue life shows that the HMA mixtures containing RAP materials possess better fatigue resistance against high pressures applied by heavy vehicles as compared to the control mixture. So, in this study, the application of RAP materials in road pavements in which freight vehicles traverse frequently is recommended. In addition, the reduction in the fatigue lives of HMA mixtures after the incorporation of RAP materials can be due to the increased stiffness of mixtures.

Effect of WMA addition As shown in Fig. 5, WMA mixtures (WC-WC50) have slightly lower fatigue lives as compared to the corresponding HMA mixtures (C-C50), which shows that the detrimental effect of WMA addition on the fatigue resistance of mixtures is extremely low. The reduction in the fatigue life of the control WMA mixture (WC) as compared to the control HMA mixture (C) was also reported by previous studies [9, 42, 43].

Sasobit® is an organic wax that is melted at temperatures above 100 °C and forms a crystalline network structure in which the interaction between the molecules of Sasobit® and functional groups of asphalt binder is improved [44]. As a result, the high-temperature properties of the asphalt binder undergo a change, and its viscosity decreases. However, the primary constituent of Sasobit® is solid paraffin, which is not liquefied at temperatures below its melting point [44]. Therefore, instead of crystalline network establishment, crystalline molecules remain active and block the free movement of asphalt binder molecules, which results in increasing the stiffness of the asphalt binder [45]. Hence, the increased stiffness of the binder causes a decrease in the fatigue resistance of mixtures.

Effect of aging As shown in Fig. 5, long-term aged HMA/WMA mixtures have shorter fatigue lives as compared to the corresponding short-term aged HMA/WMA mixtures, which is highlighted more evidently in HMA mixtures. This occurs in response to a chemical change that takes place during aging,

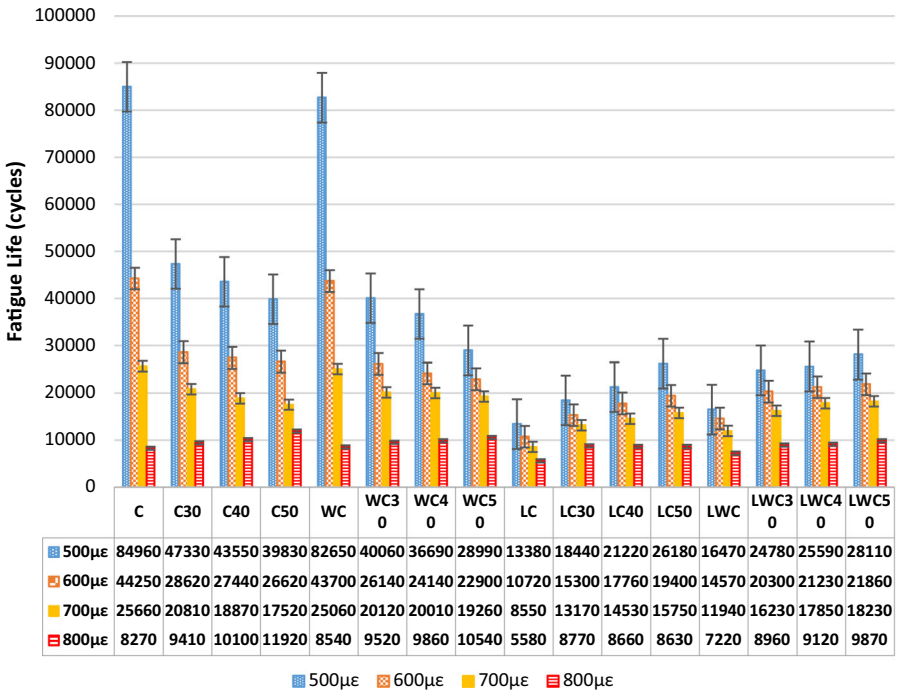

Fig. 5 The fatigue life of different compounds of mixtures

through which naphthalene aromatics are converted into polar aromatics, followed by transforming polar aromatics into asphaltene components. This results in an increase in the stiffness of binder [46].

As can be seen in Fig. 5, aging has a less adverse effect on the fatigue resistance of WMA mixtures than HMA mixtures. This indicates that the anti-aging performance of asphalt mixtures is enhanced by the addition of WMA additive in terms of fatigue resistance, which is due to a couple of reasons. First and foremost, since WMA mixtures were mixed and compacted at lower temperatures as compared to HMA mixtures, the effect of thermal aging is less significant in WMA mixtures. Second, the crystalline network structure generated in the WMA-additive modified binders establishes a dense film and protective layer over the asphalt binder, which further blocks the excessive penetration of oxygen during the aging process [44].

In this study, a relationship between fatigue lives and strain levels was found, and the results of which are shown in Fig. 6. As can be seen, strain levels are exponentially related to fatigue lives of mixtures, and the exponential-fit trendlines are drawn in Fig. 6. As can be witnessed, correlation coefficients for all types of mixtures are greater than 0.88, indicating a strong relationship between fatigue lives and strain levels, though the correlation coefficients for WMA mixtures are slightly lower than those of HMA mixtures.

As shown in Fig. 6, the sensitivity of the short-term aged control mixture to the strain levels is higher than the corresponding mixtures containing RAP materials. This shows that the addition of RAP materials affects the fatigue resistance of mixtures at lower strain levels significantly in the initial years of the service time, which results in a milder slope of the fatigue life versus strain levels' trendlines. However, the long-term fatigue performance of mixtures with RAP materials has much sensitivity to the strain levels as compared to the corresponding control mixture. This signifies that the addition of RAP materials is highly beneficial to the long-term fatigue resistance of pavements on which the vehicles with normal weights usually traverse. However, the long-term fatigue resistance of pavements on which the heavy freight vehicles normally traverse is insignificantly improved by the addition of RAP materials.

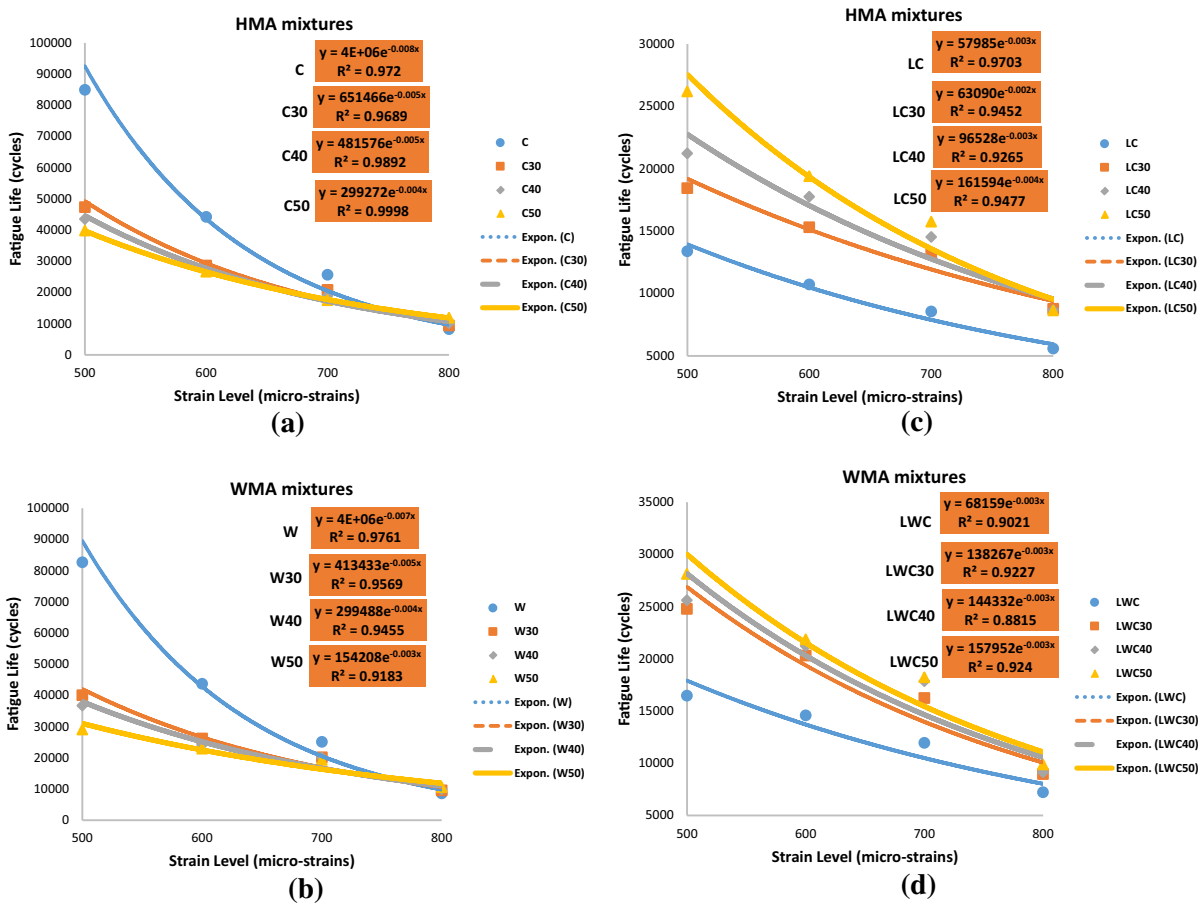

Fig. 6 Correlation between strain levels and fatigue life of different compounds of mixtures: **a** short-term aged HMA mixtures; **b** short-term aged WMA mixtures; **c** long-term aged HMA mixtures; and **d** long-term aged WMA mixtures

5.3 Statistical analysis results

In this research, the analysis of variance (ANOVA) approach is developed to investigate the experimental results. The outputs of this method comprise several parameters, including P-value and F-value. For parameters having less than 0.05 *P*-value, it shows that the considered parameters have a significant effect on the obtained results. The latter sorts out the variables based on their significance level, meaning that a higher F-value indicates a stronger impact of the parameter on the obtained results.

In order to establish this approach, a confidence level of 95% was considered. The results of the ANOVA methodology are summarized in Table 3. Based on the P-value results, temperature variations have an insignificant effect on J-integral values, as are RAP contents and warm-mix additive addition on the fracture energy (G_f) and fatigue life values. Also, long-term aging has an insignificant effect on G_f and J-integral values. Moreover, according to F-values, temperature variations, notch depths, warm-mix additive addition, and long-term aging are categorized as the most influential factors on the G_f, J-integral, and fatigue life values, respectively.

5.4 The ANFIS prediction model results

In this study, the ANFIS machine learning method was adopted to predict the fracture energy, J-integral, and fatigue life of short and long-term aged HMA/WMA mixtures containing RAP materials. Temperature variations, RAP content, the existence or the absence of WMA additive, aging level, and notch depth were considered as inputs variables for the results of the SCB test. As for the inputs variable in the 4 PB test,

Table 3 The ANOVA results for the effects of temperature, RAP content, warm-mix additive, long-term aging, strain levels, and notch depths on the fracture and fatigue resistance of mixtures

Source	Adjusted sum of squares	Adjusted mean square	F-value	*P*-value	Acceptance
G_f					
Temperature	1,089,472	544,736	11.70	0.000	Accept
RAP content	114,864	38,288	0.82	0.484	Reject
Warm-mix additive	163,603	163,603	3.52	0.063	Reject
Aging condition	613	613	0.01	0.909	Reject
Notch depth	1,106,363	553,181	11.89	0.000	Accept
J_C					
Temperature	2,669,775	1,334,888	1.80	0.179	Reject
RAP content	1,302,375	434,125	0.58	0.628	Reject
Warm-mix additive	6,543,920	6,543,920	8.81	0.005	Accept
Aging condition	266,038	266,038	0.36	0.553	Reject
N_f					
RAP content	337,174,217	112,391,406	1.13	0.345	Reject
Warm-mix additive	1,354,314	1,354,314	0.01	0.908	Reject
Aging condition	2,437,520,327	2,437,520,327	24.50	0.000	Accept
Strain level	6,234,051,805	2,078,017,268	20.88	0.000	Accept

RAP content, the existence or the absence of WMA additive, aging level, and strain level were ascertained as inputs for the results of the fatigue lives. For configuring the ANFIS model, the optimum neuro-fuzzy structure must be determined. For this, a trial-and-error process was employed to find the best structure. In this process, different types of membership function algorithms were tested and analyzed, and therefore, the optimum neuro-fuzzy structure is presented in Table 4. The adopted membership function algorithm and also the number of epochs are in agreement with a study conducted by Ziari et al. [14].

In order to reduce the data redundancy and evaluate the model precision, 70% of the fracture energy and fatigue life data set were used for training, 15% for testing, and 15% for validation. Moreover, 80% of the J-integral data set was used for training, 10% for testing, and 10% for validation. Prior to training data, the normalcy of the data set was assessed using the Kolmogorov–Smirnov test, which is in line with the method adopted by Ziari et al. [14]. In the next step, the normal data was trained using the parameters mentioned in Table 4.

Figure 7 shows the error values versus the number of epochs. As can be seen in the corresponding figure,

Table 4 Optimum neuro-fuzzy structures

Neuro-Fuzzy design	Inputs variable						Membership function algorithm	Number of epoch
	Temperature	RAP content	WMA additive	Aging	Notch depth	Strain Level		
Number of membership function								
G_f	3	4	2	1	2	–	gaussmf	100
J-integral	2	3	2	3	–	–	gaussmf	100
N_f	–	3	2	2	–	3	gaussmf	100

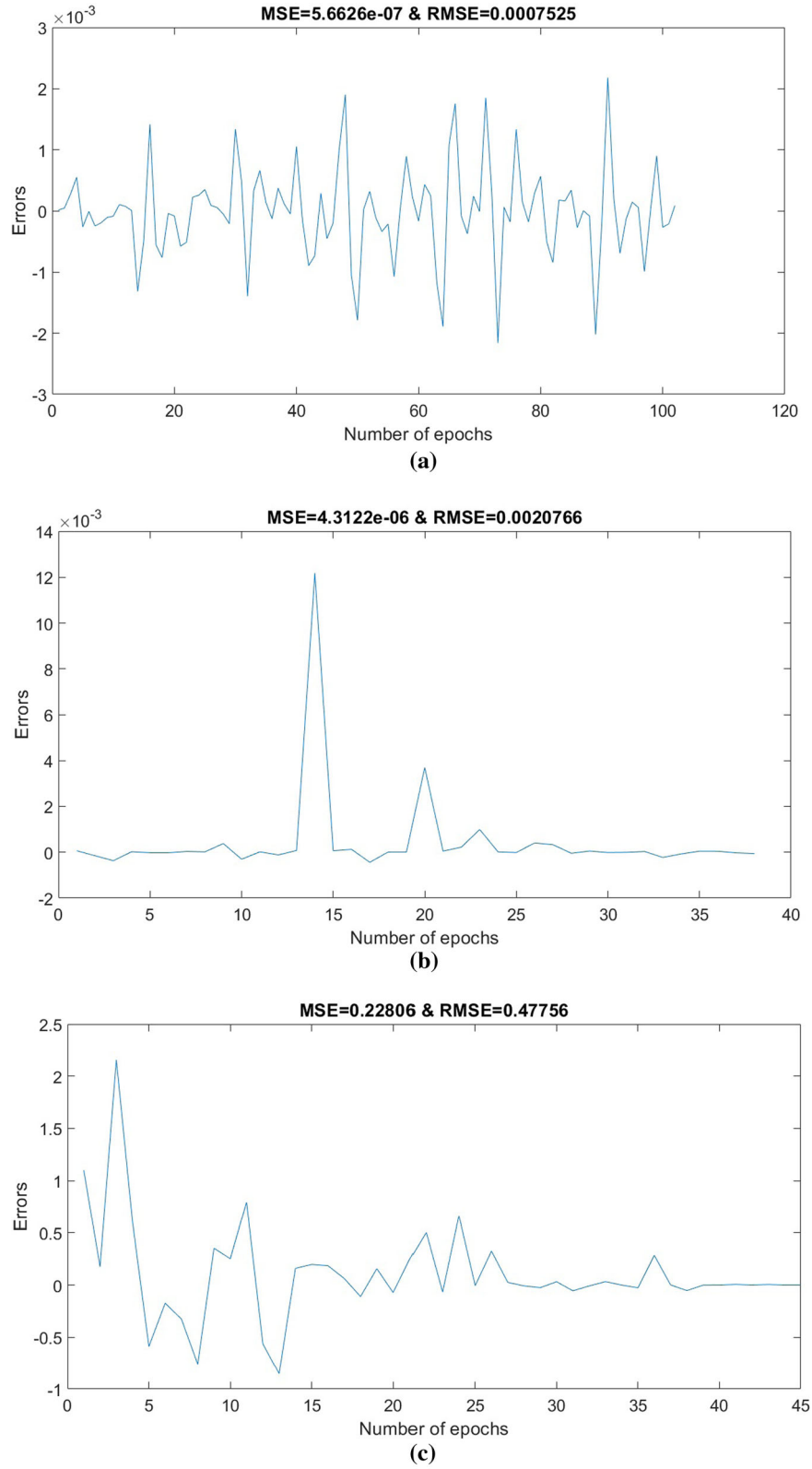

Fig. 7 Error-values versus the number of epochs: **a** fracture energy; **b** J-integral; and **c** fatigue life

the amounts of root mean square errors (RMSE) are all in low ranges for all fracture energy, J-integral, and fatigue life values, which indicates the high accuracy of the model. As can be seen in Fig. 7a, the absolute error values are in the approximate range of 0 to 0.002 J/m^2, and this fluctuation is almost consistent in epoch numbers from 0 to 100. So, it can be concluded that the adoption of epoch numbers above 100 might not be beneficial to obtain better results. As shown in Fig. 7b and c, the absolute error values become almost equal to 0 after the approximate epoch number of 37. This further implies that the considered epoch numbers were reasonable.

Figures 8, 9, and 10 show the correlation between the actual and predicted training, test, validation, and all data set. As can be seen in the corresponding figures, the correlation coefficient (R-value) for all training data is equal to 1. This shows that the ANFIS method could model the training data with perfect accuracy. Among different results, it can be seen from Fig. 8 that the precision of the ANFIS method in predicting the test and validation data of the fracture energy values is better than other parameters (i.e., J-integral and fatigue life). This shows that the more the inputs variables, the better the precision of the model. As further can be witnessed in the corresponding figures, the outlier points in the fracture energy results are much greater than the fatigue life and J-integral results. This can be explained by the fact that since the variability of the fracture energy results is

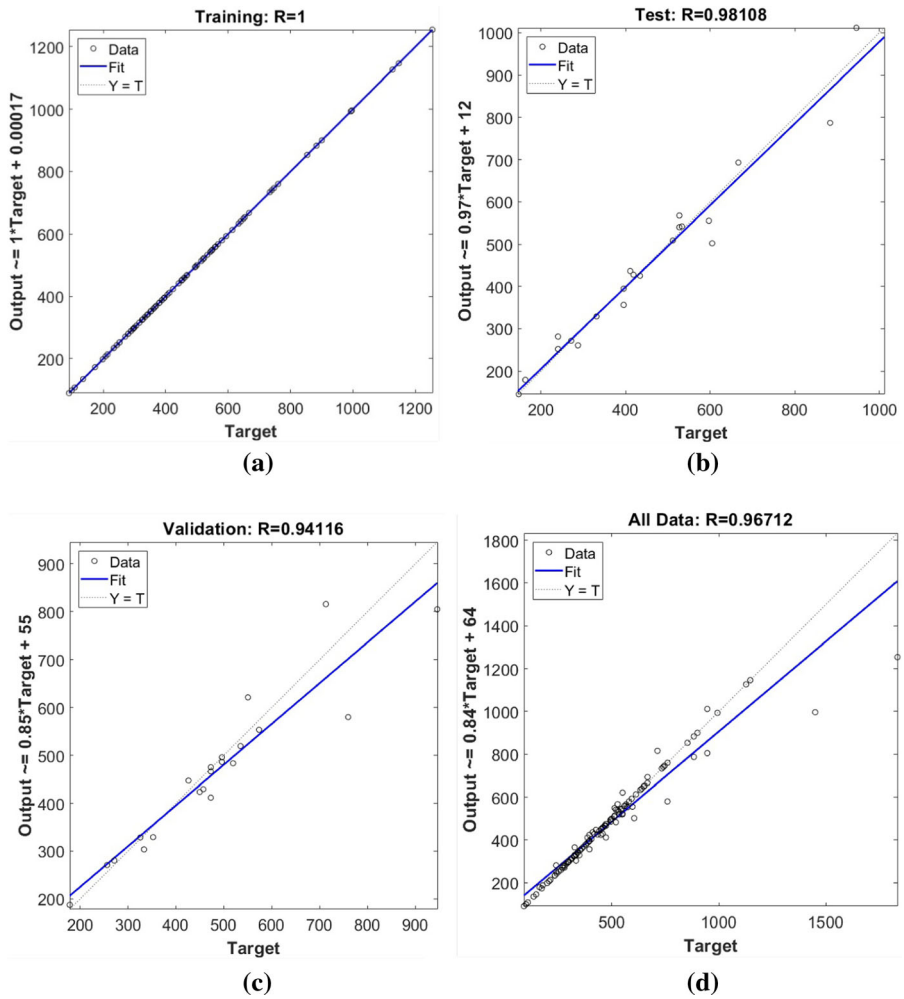

Fig. 8 The correlation between the actual and predicted fracture energy values: **a** training data; **b** test data; **c** validation data; and **d** all data

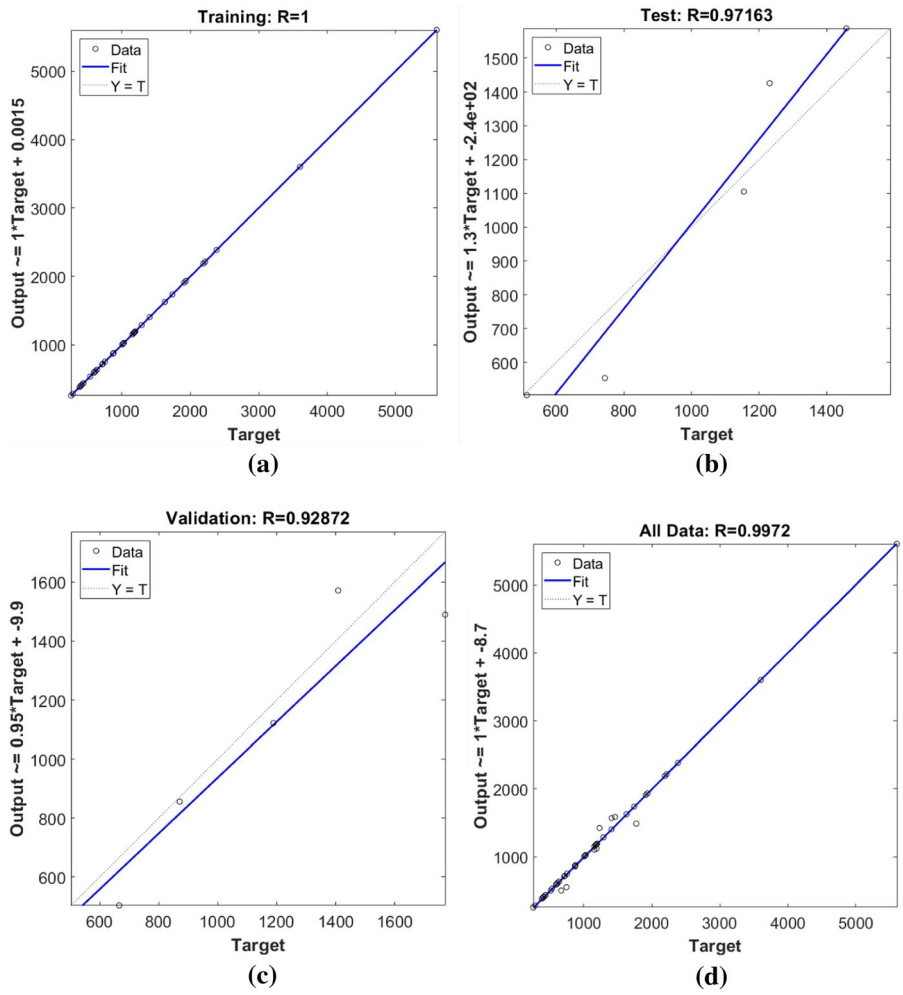

Fig. 9 The correlation between the actual and predicted J-integral values: **a** training data; **b** test data; **c** validation data; and **d** all data

higher than other parameters, the corresponding data are more scattered. It is further noted that the correlation coefficient values (R-value) for all tests, validation, and all data set of fracture energy, J-integral, and fatigue life values are greater than 0.9. This shows that the ANFIS model was able to test and validate the data set with an acceptable accuracy [15].

Root mean square error (RMSE) is used to characterize the model prediction ability. Table 5 shows the RMSE values of different results for all data types. As can be seen, the ANFIS method could model the training data with great precision. It is further noted that the ANFIS method could model the fatigue life with lower precision as compared to the fracture energy and J-integral. This is due to the fact that, as discussed previously, the trend for fatigue lives changes immediately after the strain level of 800 $\mu\varepsilon$, which results in a lower ability of this model to distinguish the inflection point. With regard to the ranking of the model precision, the fracture energy ranks the best, followed by the J-integral and fatigue life.

6 Conclusions

In this research, the fracture and fatigue resistance of short and long-term aged HMA/WMA mixtures containing 0%, 30%, 40%, and 50% RAP materials were investigated. In addition, the ANFIS machine learning method was adopted to predict the fracture

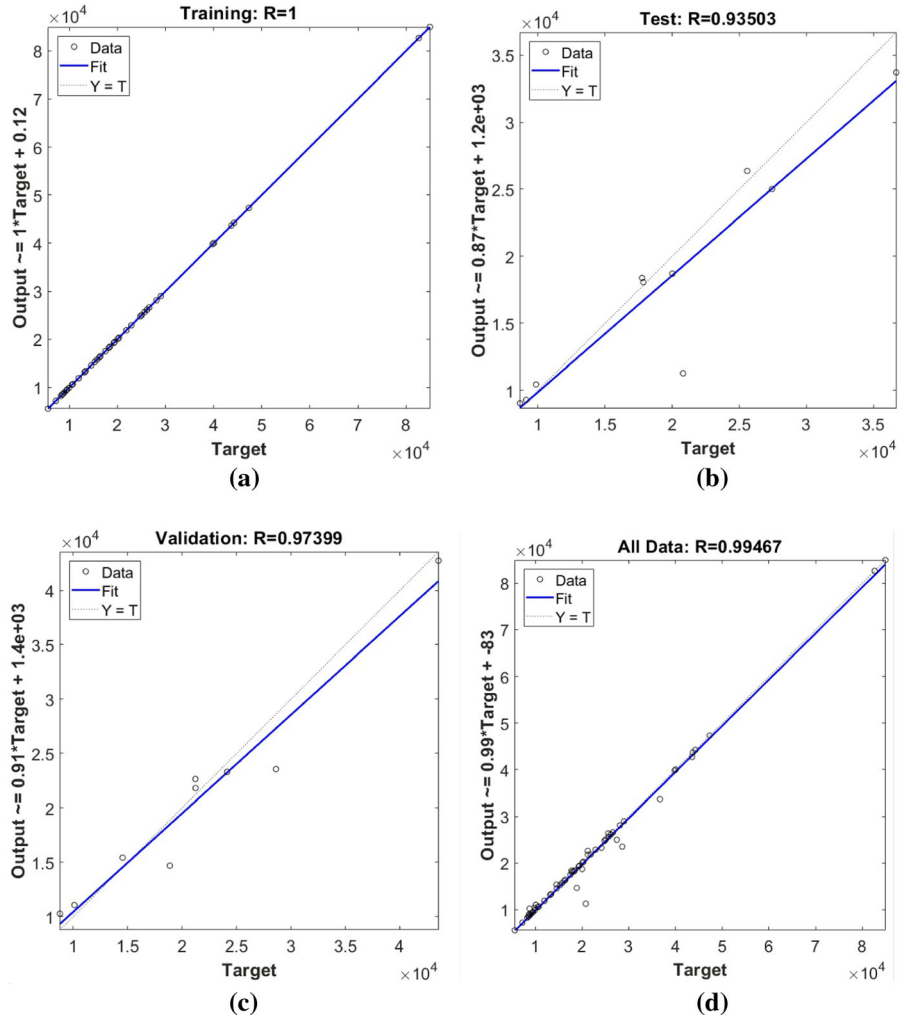

Fig. 10 The correlation between the actual and predicted fatigue life values: **a** training data; **b** test data; **c** validation data; and **d** all data

Table 5 RMSE values of different parameters

Data type	Root mean square error (RMSE)		
	Fracture energy	J-integral	Fatigue life
Training	0.0007	0.0021	0.4776
Test	40.0284	136.7932	219.8362
Validation	60.6170	165.5229	158.4222
All	67.5416	69.3047	105.2644

and fatigue test outputs. The conclusions based on the test results can be summed up as follows:

- It was observed that the addition of RAP materials into HMA mixtures decreased the fracture resistance at 0 °C and − 20 °Cand fatigue resistance at strain levels below 800 με as compared to the control mixture, whereas the fracture resistance was enhanced at 20 °Cand the fatigue resistance was also improved at strain level above 800 $\mu\varepsilon$.
- It was concluded that the addition of WMA additive generally deteriorated the fracture resistance of mixtures, with the only exception that its addition into mixtures with 50% RAP materials improved the fracture resistance. Also, WMA mixtures had slightly lower fatigue resistance as compared to HMA mixtures.

- Although the long-term aging reduced the fracture resistance of all HMA mixtures, the aging resistance of HMA mixtures with RAP materials was better than the control mixture in terms of fracture resistance. Interestingly, the fracture resistance of long-term aged WMA mixtures was better than the corresponding short-term aged WMA mixtures. Furthermore, the anti-aging properties of WMA mixtures were better than HMA mixtures in terms of fatigue resistance.
- Based on the ANFIS results, it was observed that this method could model the fracture and fatigue properties of asphalt mixtures with great precision. Among different parameters, the ANFIS method had a much better ability to predict the fracture energy values.

In general, the results of this study suggested that the use of WMA additive in combination with high RAP contents is advantageous to the low-temperature cracking resistance of pavements in cold regions, and it does not have a significant effect on fatigue resistance. In addition, the WMA additive is suggested to be used in pavements subjected to excessive aging conditions. This is because it improves the aging resistance of asphalt pavements. Also, the incorporation of RAP materials into asphalt mixtures improves the intermediate cracking and fatigue resistance at higher strain levels, and it is favorable for improving the anti-aging properties of asphalt mixtures. So, the use of RAP materials in pavements subjected to heavy loads is favorable to extend the fatigue life.

Declarations

Conflict of interest The authors declare that they have no conflict of interest.

References

1. Yousefi AA, Sobhi S, Aliha MRM, Pirmohammad S, Haghshenas HF (2021) Cracking properties of warm mix asphalts containing reclaimed asphalt pavement and recycling agents under different loading modes. Constr Build Mater 300:124130. https://doi.org/10.1016/j.conbuildmat.2021.124130
2. Majidifard H, Tabatabaee N, Buttlar W (2019) Investigating short-term and long-term binder performance of high-RAP mixtures containing waste cooking oil. J Traffic Transp Eng 6(4):396–406. https://doi.org/10.1016/j.jtte.2018.11.002
3. Zhang J, Guo C, Chen T, Zhang W, Yao K, Fan C, Liang M, Guo C, Yao Z (2020) Evaluation on the mechanical performance of recycled asphalt mixtures incorporated with high percentage of RAP and self-developed rejuvenators. Constr Build Mater 121337
4. Goli H, Latifi M (2020) Evaluation of the effect of moisture on behavior of warm mix asphalt (WMA) mixtures containing recycled asphalt pavement (RAP). Constr Build Mater 247:118526
5. Kamboozia N, Saed SA, Rad SM (2021) Rheological behavior of asphalt binders and fatigue resistance of SMA mixtures modified with nano-silica containing RAP materials under the effect of mixture conditioning. Constr Build Mater 303:124433. https://doi.org/10.1016/j.conbuildmat.2021.124433
6. Ziari H, Aliha M, Moniri A, Saghafi Y (2020) Crack resistance of hot mix asphalt containing different percentages of reclaimed asphalt pavement and glass fiber. Constr Build Mater 230:117015
7. Yousefi A, Behnood A, Nowruzi A, Haghshenas H (2020) Performance evaluation of asphalt mixtures containing warm mix asphalt (WMA) additives and reclaimed asphalt pavement (RAP). Constr Build Mater 121200
8. Saed SA, Kamboozia N, Rad SM (2021) Performance evaluation of stone matrix asphalt mixtures and low-temperature properties of asphalt binders containing reclaimed asphalt pavement materials modified with nanosilica. J Mater Civ Eng (in press)
9. Goh SW, You Z (2011) Evaluation of warm mix asphalt produced at various temperatures through dynamic modulus testing and four point beam fatigue testing. Pavements Mater Recent Adv Design Test Constr p 123–30
10. Sobhi S, Yousefi A, Behnood A (2020) The effects of Gilsonite and Sasobit on the mechanical properties and durability of asphalt mixtures. Constr Build Mater 238:117676
11. Rodríguez-Alloza AM, Gallego J (2017) Mechanical performance of asphalt rubber mixtures with warm mix asphalt additives. Mater Struct 50(2):1–9
12. Lu DX, Saleh M (2016) Laboratory evaluation of warm mix asphalt incorporating high RAP proportion by using evotherm and sylvaroad additives. Constr Build Mater 114:580–587. https://doi.org/10.1016/j.conbuildmat.2016.03.200
13. Guo M, Liu H, Jiao Y, Mo L, Tan Y, Wang D, Liang M (2020) Effect of WMA-RAP technology on pavement performance of asphalt mixture: a state-of-the-art review. J Clean Prod 121704
14. Ziari H, Amini A, Moniri A, Habibpour M (2020) Using the GMDH and ANFIS methods for predicting the crack resistance of fibre reinforced high RAP asphalt mixtures. Road Mater Pavement Design 1–19
15. Alas M, Ali SIA, Abdulhadi Y, Abba S (2020) Experimental evaluation and modeling of polymer nanocomposite modified asphalt binder using ANN and ANFIS. J Mater Civ Eng 32(10):04020305
16. AASHTO (2017) Standard specification for stone matrix asphalt (SMA). Washington, DC: AASHTO: AASHTO M325–08
17. ASTM (2017) Standard test methods for quantitative extraction of asphalt binder from asphalt mixtures. West Conshohocken, PA: ASTM: ASTM D2172M-17

18. ASTM (2017) Standard practice for recovery of asphalt from solution using the rotary evaporator. ASTM International: ASTM D5404M-12
19. Kamboozia N, Rad SM, Saed SA (2021) Laboratory investigation of the effect of nano-ZnO on the fracture and rutting resistance of porous asphalt mixture under the aging condition and freeze-thaw cycle. J Mater Civ Eng (In Press)
20. Ameli A, Nasr D, Babagoli R, Pakshir AH, Norouzi N, Davoudinezhad S (2020) Laboratory evaluation of rheological behavior of binder and performance of stone matrix asphalt (SMA) mixtures containing zycotherm nanotechnology, sasobit, and rheofalt warm mixture additives. Constr Build Mater 262:120757
21. Xu J, Yang E, Luo H, Ding H (2020) Effects of warm mix additives on the thermal stress and ductile resistance of asphalt binders. Constr Build Mater 238:117746
22. Ameri M, Yazdipanah F, Yengejeh AR, Afshin A (2020) Production temperatures and mechanical performance of rubberized asphalt mixtures modified with two warm mix asphalt (WMA) additives. Mater Struct 53(4):1–16
23. AASHTO (2019) Standard method of test for viscosity determination of asphalt binder using rotational viscometer. Washington, DC: AASHTO T316–19
24. Pirmohammad S, Khanpour M (2020) Fracture strength of warm mix asphalt concretes modified with crumb rubber subjected to variable temperatures. Road Mater Pavement Design 1–19
25. Sedaghat B, Taherrian R, Hosseini SA, Mousavi SM (2020) Rheological properties of bitumen containing nanoclay and organic warm-mix asphalt additives. Constr Build Mater 243:118092
26. AASHTO (2015) Standard method of test for resistance to plastic flow of bituminous mixtures using marshall apparatus. Washington, DC: AASHTO: AASHTO T245–15
27. AASHTO (2017) Standard practice for designing stone matrix asphalt (SMA). Washington, DC: AASHTO: AASHTO R 46–08
28. AASHTO (2019) Standard practice for mixture conditioning of hot-mix asphalt (HMA). Washington, DC: AASHTO R30–02
29. ASTM (2016) Standard test method for evaluation of asphalt mixture cracking resistance using the semi-circular bend test (SCB) at Intermediate temperatures. West Conshohocken, PA: ASTM: ASTM D8044–16
30. AASHTO (2017) Standard method of test for determining the fatigue life of compacted asphalt mixtures subjected to repeated flexural bending Washington, DC: AASHTO T321
31. Behnia B, Dave EV, Ahmed S, Buttlar WG, Reis H (2011) Effects of recycled asphalt pavement amounts on low-temperature cracking performance of asphalt mixtures using acoustic emissions. Transp Res Rec 2208(1):64–71
32. Singh D, Ashish PK, Chitragar SF (2018) Laboratory performance of recycled asphalt mixes containing wax and chemical based warm mix additives using semi circular bending and tensile strength ratio tests. Constr Build Mater 158:1003–1014
33. Moniri A, Ziari H, Aliha M, Saghafi Y (2019) Laboratory study of the effect of oil-based recycling agents on high RAP asphalt mixtures. Int J Pavement Eng 1–12
34. Wang H, Wang J, Chen J (2014) Micromechanical analysis of asphalt mixture fracture with adhesive and cohesive failure. Eng Fract Mech 132:104–119
35. Wasiuddin NM, Zaman MM, O'Rear EA (2008) Effect of sasobit and aspha-min on wettability and adhesion between asphalt binders and aggregates. Transp Res Rec 2051(1):80–89
36. Zhang J, Yang F, Pei J, Xu S, An F (2015) Viscosity-temperature characteristics of warm mix asphalt binder with Sasobit®. Constr Build Mater 78:34–39
37. Guo N, You Z, Zhao Y, Tan Y, Diab A (2014) Laboratory performance of warm mix asphalt containing recycled asphalt mixtures. Constr Build Mater 64:141–149
38. Li B, Yang J, Li X, Liu X, Han F, Li L (2015) Effect of short-term aging process on the moisture susceptibility of asphalt mixtures and binders containing sasobit warm mix additive. Adv Mater Sci Eng 2015
39. Ziari H, Moniri A, Bahri P, Saghafi Y (2019) The effect of rejuvenators on the aging resistance of recycled asphalt mixtures. Constr Build Mater 224:89–98
40. Hamedi GH, Saedi D, Ghahremani H (2020) Effect of short-term aging on low-temperature cracking in asphalt mixtures using mechanical and thermodynamic methods. J Mater Civ Eng 32(10):04020288
41. Bharath G, Reddy KS, Tandon V, Reddy MA (2021) Aggregate gradation effect on the fatigue performance of recycled asphalt mixtures. Road Mater Pavement Design 22(1):165–184
42. Haggag MM, Mogawer WS, Bonaquist R (2011) Fatigue evaluation of warm-mix asphalt mixtures: use of uniaxial, cyclic, direct tension compression test. Transp Res Rec 2208(1):26–32
43. Alinezhad M, Sahaf A (2019) Investigation of the fatigue characteristics of warm stone matrix asphalt (WSMA) containing electric arc furnace (EAF) steel slag as coarse aggregate and Sasobit as warm mix additive. Case Stud Construct Mater 11:e00265
44. Liu H, Zhang Z, Xie J, Gui Z, Li N, Xu Y (2021) Analysis of OMMT strengthened UV aging-resistance of Sasobit/SBS modified asphalt: Its preparation, characterization and mechanism. J Clean Prod 315:128139. https://doi.org/10.1016/j.jclepro.2021.128139
45. Harooni Jamaloei M, Aboutalebi Esfahani M, Filvan TM (2019) Rheological and mechanical properties of bitumen modified with Sasobit, polyethylene, paraffin, and their mixture. J Mater Civ Eng 31(7):04019119
46. Behnood A (2019) Application of rejuvenators to improve the rheological and mechanical properties of asphalt binders and mixtures: a review. J Clean Prod 231:171–182. https://doi.org/10.1016/j.jclepro.2019.05.209